

# Study of $e^+e^-$ collisions with a hard initial state photon at *BABAR*

Michel Davier<sup>a</sup>

E-mail: davier@lal.in2p3.fr

<sup>a</sup>Laboratoire de l'Accélérateur Linéaire, IN2P3/CNRS-Université de Paris-Sud,  
BP34, 91898 Orsay, France

A study of several 3- and 4-body hadronic final states ( $\pi^+\pi^-\pi^0$ ,  $\pi^+\pi^-\pi^+\pi^-$ ,  $K^+K^-\pi^+\pi^-$  and  $K^+K^-K^+K^-$ ) accompanied by a hard photon is presented. These states are produced from  $e^+e^-$  collisions at the c.m. energy near the  $\Upsilon(4S)$  resonance using a  $90\text{ fb}^{-1}$  data sample collected with the *BABAR* detector at the PEP-II collider. The invariant mass of the hadronic final state determines the virtual photon energy, so that the data can be compared with direct  $e^+e^-$  cross sections. Cross sections have been obtained from threshold up to 4.5 GeV with systematic errors at the 5% level. The accuracy of the results is comparable with the best direct  $e^+e^-$  results overall, but achieves much better precision in 1.4-2.5 GeV region where data are sparse. In addition to light meson spectroscopy these data can be used to improve the determination of  $R$  –the ratio of  $e^+e^- \rightarrow$  hadrons cross section to  $e^+e^- \rightarrow \mu^+\mu^-$ – and thereby to impact the understanding of the recent  $(g-2)_\mu$  measurement through a better evaluation of the hadronic vacuum polarization contribution. The ISR technique also gives access to  $J/\psi$  production and allows one to measure branching ratios into 3- and 4-body final states above at a level of precision that is typically better than that obtained in the combined earlier measurements.

## 1. Introduction

The possibility of using the initial state radiation (ISR) of hard photons at B-factories to study hadronic final state production at lower  $e^+e^-$  c.m. energies has been discussed previously [1-3]. The interest in this kind of study has been increasing because of the discrepancy between the measured muon  $g-2$  value and the prediction within the Standard Model [4,5], where the hadronic vacuum polarization contribution is evaluated using data from  $e^+e^-$  experiments at low energies. The study of ISR events at B-factories can provide independent measurements of hadronic cross sections as well as contribute to hadronic spectroscopy.

The ISR cross section for a particular final state  $f$  depends on  $e^+e^-$  cross section  $\sigma_f(s)$  and is obtained from:

$$\frac{d\sigma(s, x)}{dx} = W(s, x) \cdot \sigma_f(s(1-x)), \quad (1)$$

where  $x = 2E_\gamma/\sqrt{s}$ ,  $E_\gamma$  is the energy of the ISR photon in the nominal c.m. frame with total energy  $\sqrt{s}$ , and  $s' = s(1-x)$  is the square of the mass of the produced  $f$  state. The function

$W(s, x)$  describes the energy spectrum of the virtual photons and can be calculated with better than 1% accuracy [1-3]. ISR photons are produced at all angles relative to the collision axis. The *BABAR* acceptance for such photons at relatively large angles (typically  $20$ - $144^\circ$  in the laboratory frame) is around 10-15 %.

An advantage deriving from the use of ISR is that the entire range of effective collision energy is scanned in one experiment. This avoids the relative normalization uncertainties which can arise when data from different experiments are combined. A disadvantage is that the invariant mass resolution is a limit when studying narrow resonances.

A comprehensive program is under way at *BABAR* to measure all hadronic processes in the few GeV range. While the  $\pi^+\pi^-$  channel requires more systematic studies in order to reach the interesting 1% (or better) level, some results are already available for 2- and 3-body processes with lower cross sections. They are presented in this contribution.

The ISR method gives also access to  $J/\psi$  de-

cays. The cross section for the final state  $f$

$$\sigma_{J/\psi}^f(s) = \frac{12\pi^2 \Gamma_{ee} B_f}{m_{J/\psi} s} W(s, x), \quad (2)$$

with  $x = 1 - m_{J/\psi}^2/s$ , is proportional to the product  $\Gamma_{ee} \cdot B_f$  or  $\Gamma \cdot B_{ee} \cdot B_f$  where  $\Gamma$  and  $B_{ee}$ ,  $B_f$  are the total width and branching fractions of  $J/\psi$  into  $e^+e^-$  and  $f$ . The invariant mass of the final particles determines the position of the  $J/\psi$  peak and a detector mass resolution  $\sim 8$  MeV can be achieved by using a kinematic fit. Preliminary studies of some particular ISR processes have been performed (see Ref. [6-8]) showing good *BABAR* detector[9] efficiency and particle identification capability for these types of events. Signal and background ISR processes are simulated using Monte Carlo (MC) event generators based on computer codes described in Ref. [10-13]. Also simulated were generic background from quark-antiquark and  $\tau\bar{\tau}$  processes using JETSET [14] and KORALB [15] packages.

## 2. Three-body final state: $\pi^+\pi^-\pi^0$

The initial selection of  $e^+e^- \rightarrow \pi^+\pi^-\pi^0\gamma$  candidates requires that all the final particles are detected inside a fiducial volume. One of the photons is required to have an energy in the c.m. frame above 3 GeV. Two of the tracks must originate from the interaction point, have a transverse momentum above 100 MeV/c with no kaon-ID and be in the good region of detector acceptance. The photon with greatest c.m. energy is assumed to be the ISR photon. The remaining photons are paired to form candidate  $\pi^0$ s. A kinematic fit is applied to the selected event, imposing energy and momentum conservation, and constraining the candidate  $\pi^0$  invariant mass. Analysis details can be found in Ref. [8]. The  $3\pi$  invariant mass distribution of the events after background subtraction was fit with a sum of excitation curves describing  $\omega(782), \phi(1020), \omega(1420)$  and  $\omega(1650)$  resonances. Relative phases for  $\omega(1420)$  and  $\omega(1650)$  are fixed at 0 and  $\pi$ . The resulting parameters obtained from the fit (Fig. 1,  $\chi^2/\text{dof} = 146/148$ ) are the following:

$$\mathcal{B}_{\omega ee} \mathcal{B}_{\omega 3\pi} = (6.70 \pm 0.06 \pm 0.27) 10^{-5} \quad (3)$$

$$\begin{aligned} \mathcal{B}_{\phi ee} \mathcal{B}_{\phi 3\pi} &= (4.30 \pm 0.08 \pm 0.21) 10^{-5} \\ \mathcal{B}_{\omega' ee} \mathcal{B}_{\omega' 3\pi} &= (0.82 \pm 0.05 \pm 0.06) 10^{-6} \\ M_{\omega'} &= (1350 \pm 20 \pm 20) \text{ MeV}/c^2 \\ \Gamma_{\omega'} &= (450 \pm 70 \pm 70) \text{ MeV}/c^2 \\ \mathcal{B}_{\omega'' ee} \mathcal{B}_{\omega'' 3\pi} &= (1.3 \pm 0.1 \pm 0.1) 10^{-6} \\ M_{\omega''} &= (1660 \pm 10 \pm 2) \text{ MeV}/c^2 \\ \Gamma_{\omega''} &= (230 \pm 30 \pm 20) \text{ MeV}/c^2 \end{aligned} \quad (4)$$

The fitted masses and widths of the  $\omega'$  and  $\omega''$  mesons are model dependent but nevertheless can be compared with the estimates of these parameters by the PDG [16]:  $M_{\omega'} = 1400 - 1450 \text{ MeV}/c^2$ ,  $\Gamma_{\omega'} = 180 - 250 \text{ MeV}/c^2$ ,  $M_{\omega''} = 1670 \pm 30 \text{ MeV}/c^2$ ,  $\Gamma_{\omega''} = 315 \pm 35 \text{ MeV}/c^2$ . The PDG data are based on small data samples for  $e^+e^- \rightarrow \omega', \omega'' \rightarrow 3\pi$ ,  $\omega\pi\pi$  [21,20,23],  $p\bar{p} \rightarrow \omega'\pi^0 \rightarrow \omega\pi^0\pi^0\pi^0$  [17], and  $\pi^-p \rightarrow \omega''n \rightarrow \omega\eta n$  [18] reactions. We present a new measurement of the  $\omega'$  and  $\omega''$  parameters based on a significantly larger data sample for the  $e^+e^- \rightarrow \omega', \omega'' \rightarrow 3\pi$  reaction. From the measured values of  $\mathcal{B}(V \rightarrow e^+e^-)\mathcal{B}(V \rightarrow 3\pi)$ , the electronic widths of  $\omega'$  and  $\omega''$  can be estimated. Assuming that  $\mathcal{B}(\omega' \rightarrow 3\pi) \approx 1$  and  $\mathcal{B}(\omega'' \rightarrow 3\pi) \approx 0.5$  we derive that  $\Gamma(\omega' \rightarrow e^+e^-) \approx 370 \text{ eV}$  and  $\Gamma(\omega'' \rightarrow e^+e^-) \approx 570 \text{ eV}$ . The large values of these widths, comparable with  $\Gamma(\omega \rightarrow e^+e^-) \approx 600 \text{ eV}$ , are in disagreement with expectations of the quark model, which predicts at least one order of magnitude lower values for the electronic widths for the excited meson states (see, for example, Ref. [19]).

The  $e^+e^- \rightarrow \pi^+\pi^-\pi^0$  cross section in the 1.05-3.0 GeV/ $c^2$  region is presented in Fig. 2. It is in agreement with the SND data [20], but it shows a large discrepancy with the DM-2 [21] measurement.

It is interesting to plug these new results into the dispersion integral yielding the corresponding vacuum polarization contribution to the muon anomalous magnetic moment. In order to compare with previous calculations [4] using existing data, the energy interval 1.055 to 1.8 GeV is chosen. The current value [4] is

$$a_\mu^{\text{had}} = (2.45 \pm 0.26_{\text{exp}} \pm 0.03_{\text{rad}}) 10^{-10} \quad (5)$$

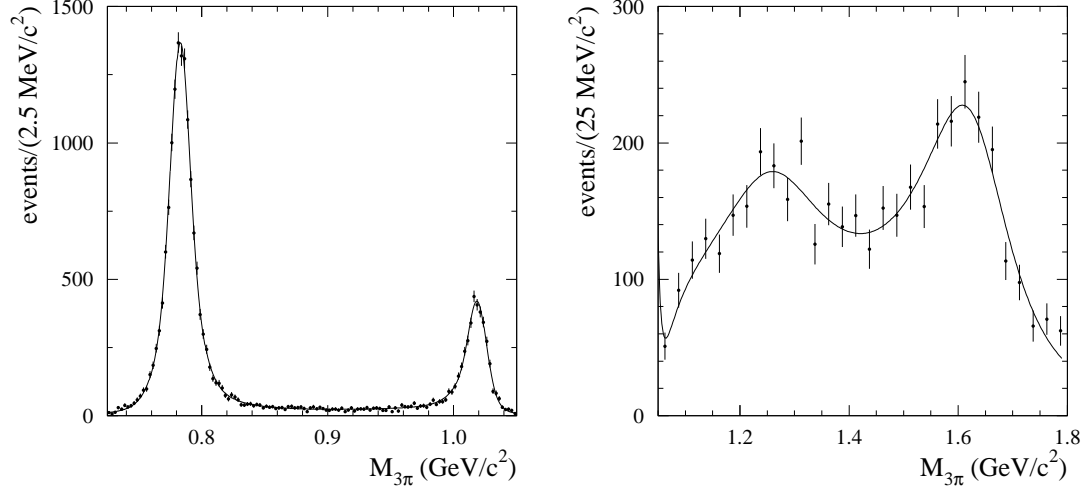


Figure 1. The background-subtracted  $3\pi$  mass spectrum for masses between 0.70 and 1.05  $\text{GeV}/c^2$  (left) and for masses from 1.05 to 1.80  $\text{GeV}/c^2$  (right). The curves are the result of the fit.

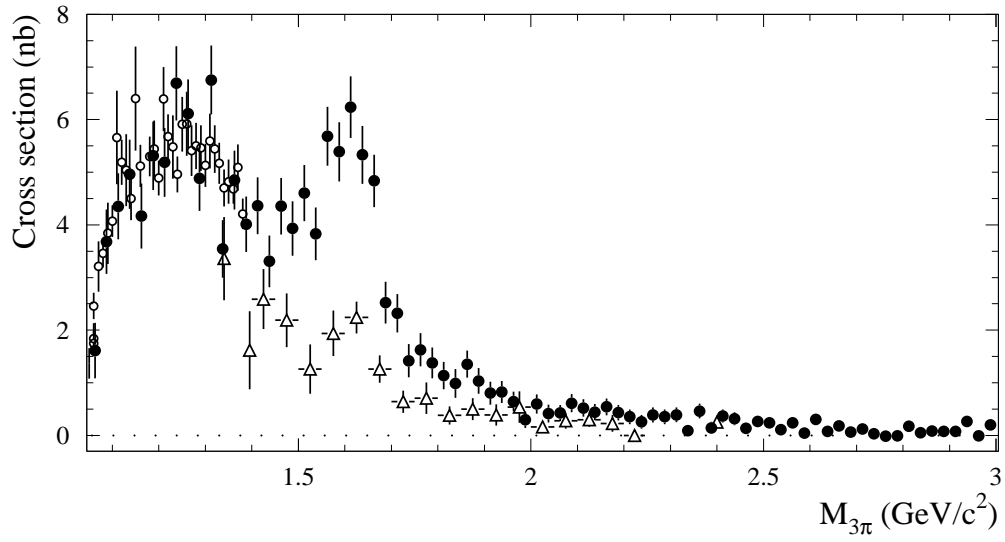


Figure 2. The  $e^+e^- \rightarrow \pi^+\pi^-\pi^0$  cross section measured in this work (filled circles), by SND (open circles), and DM2 (open triangles).

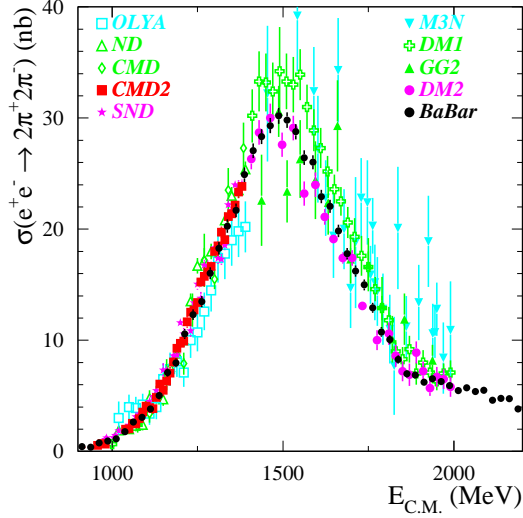


Figure 3. The  $e^+e^- \rightarrow \pi^+\pi^-\pi^+\pi^-$  cross section obtained from ISR at *BABAR* in comparison with existing  $e^+e^-$  data.

while the new estimate using only the new *BABAR* data yields a larger and more precise contribution,

$$a_\mu^{had} = (3.31 \pm 0.13_{exp} \pm 0.03_{rad})10^{-10} \quad (6)$$

### 3. Four-body final states: $\pi^+\pi^-\pi^+\pi^-$ , $K^+K^-\pi^+\pi^-$ and $K^+K^-K^+K^-$

Event candidates were required to have four good charged tracks and a hard photon assumed to be from ISR. Hadron identification in *BABAR* is used to separate charged pions from kaons and identify the different  $\pi^+\pi^-\pi^+\pi^-$ ,  $K^+K^-\pi^+\pi^-$  and  $K^+K^-K^+K^-$  final states is described. Figure 3 presents the obtained  $e^+e^- \rightarrow \pi^+\pi^-\pi^+\pi^-$  cross section in comparison with all existing  $e^+e^-$  data. The estimated systematic error is about 5%.

Again we can examine the impact of these new results on the calculation of hadronic vacuum polarization. The hadronic contribution to  $(g-2)_\mu$  from the  $\pi^+\pi^-\pi^+\pi^-$  channel [4], evaluated using all available  $e^+e^-$  or  $\tau$  decay data in 0.56-1.8 GeV

range is

$$a_\mu^{had,ee} = (14.21 \pm 0.87_{exp} \pm 0.23_{rad})10^{-10} \quad (7)$$

$$a_\mu^{had,\tau} = (12.35 \pm 0.96_{exp} \pm 0.40_{SU2})10^{-10} \quad (8)$$

The  $\tau$  evaluation is less precise in this channel since it is based on the measurement of the spectral function in the  $\tau \rightarrow \nu_\tau \pi 3\pi^0$  decay mode, involving the reconstruction of three  $\pi^0$  decays.

Evaluating the same contribution with the *BABAR* data in this energy range gives

$$a_\mu^{had} = (12.95 \pm 0.64_{exp} \pm 0.13_{rad}) 10^{-10} \quad (9)$$

which shows the potential of ISR measurements.

Figure 4 shows the obtained cross sections for  $K^+K^-\pi^+\pi^-$  and  $K^+K^-K^+K^-$  final states. The systematic normalization errors are 15% and 25%, coming essentially from the uncertainties in the dynamics used in the Monte Carlo event generators. respectively.

### 4. Three- and four-body $J/\psi$ decays

The invariant mass of three pions from  $J/\psi$  decays is shown in Fig. 5(top). From about 900 events after background subtraction the following product can be determined:

$$\Gamma(J/\psi \rightarrow e^+e^-)\mathcal{B}(J/\psi \rightarrow 3\pi) = (122 \pm 5 \pm 8) \text{ eV} \quad (10)$$

The systematic error includes the uncertainties on the detection efficiency, the integrated luminosity, and the radiative correction. Using the  $\Gamma(J/\psi \rightarrow e^+e^-)$  measurement obtained by *BABAR* [7] from the study of  $e^+e^- \rightarrow J/\psi\gamma$  with  $J/\psi \rightarrow \mu^+\mu^-$ , the  $J/\psi \rightarrow 3\pi$  branching fraction is calculated to be

$$\mathcal{B}(J/\psi \rightarrow 3\pi) = (2.18 \pm 0.19)\% \quad (11)$$

which is in substantial disagreement ( $\sim 3\sigma$ ) with the world average value [16] of  $(1.47 \pm 0.13)\%$ , but agrees with the recent result from BES [22]:  $\mathcal{B}(J/\psi \rightarrow 3\pi) = (2.10 \pm 0.12)\%$ .

Figure 5 shows the  $J/\psi$  and  $\psi(2S)$  signals (containing  $270 \pm 20$  and  $620 \pm 25$  observed events respectively) in the four-charged-track invariant mass spectrum. The latter signal originates from the process  $\psi(2S) \rightarrow J/\psi \pi^+\pi^- \rightarrow \mu\mu\pi^+\pi^-$  and can be easily isolated by requiring the mass of one

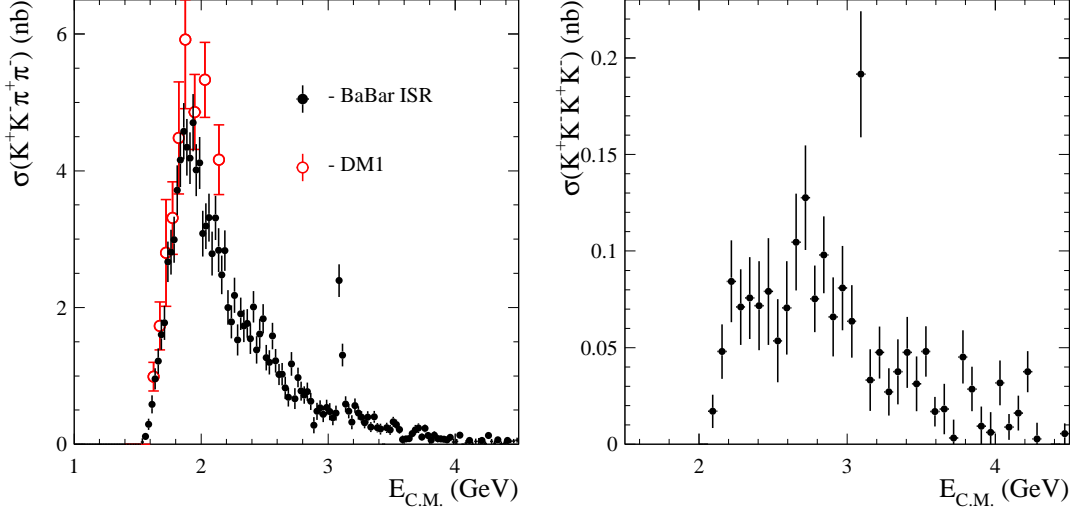


Figure 4. The  $e^+e^- \rightarrow K^+K^-\pi^+\pi^-$  (left) and  $K^+K^-K^+K^-$  (right) cross sections obtained from ISR at *BABAR* in comparison with  $e^+e^-$  data.

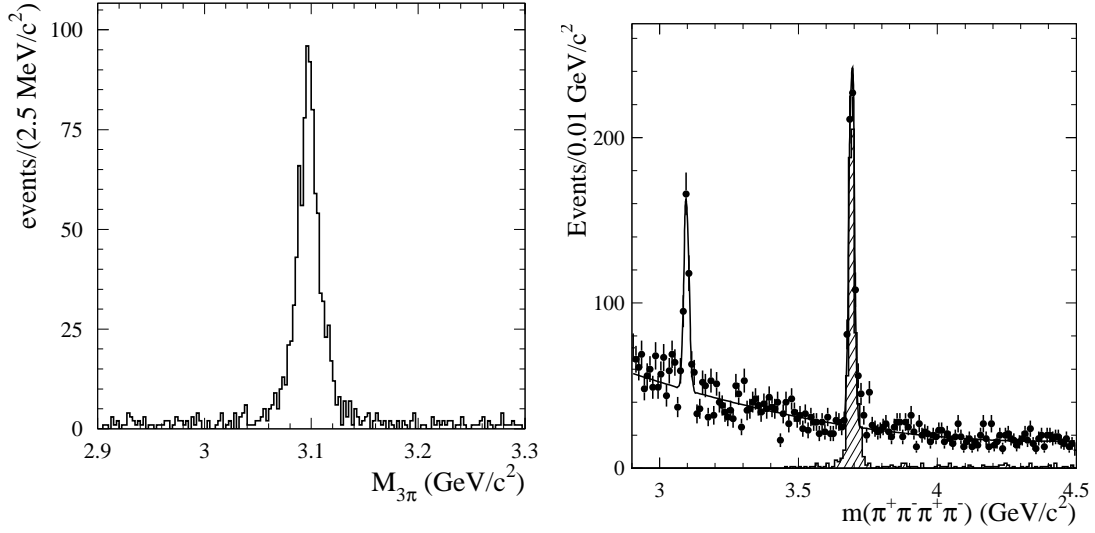


Figure 5. The signals from  $J/\psi$  and  $\psi(2S)$  in  $3\pi$ (left) and  $4\pi$ (right) final states. The shaded region at the latter corresponds to  $\psi(2S) \rightarrow J/\psi\pi^+\pi^-$ , with  $J/\psi \rightarrow \mu^+\mu^-$ .

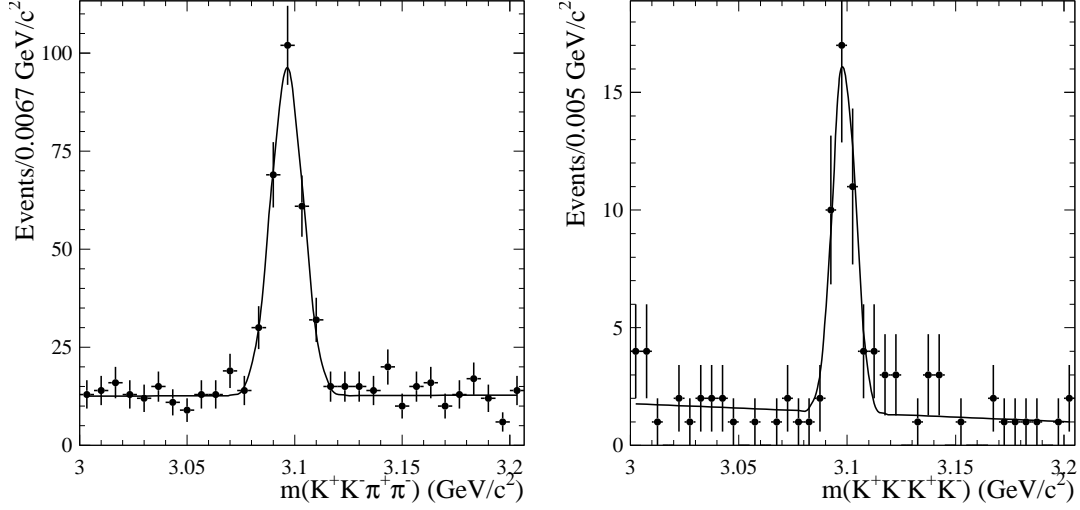


Figure 6. The signals from  $J/\psi$  decays into  $K^+K^-\pi^+\pi^-$  (left) and  $K^+K^-K^+K^-$  (right) final states.

pair of charged particles (shaded histogram) to be consistent with the  $J/\psi$  mass. By using detection efficiency from simulation and the effective ISR luminosity the following products have been obtained:

$$\begin{aligned} \mathcal{B}_{J/\psi \rightarrow 4\pi} \cdot \Gamma_{J/\psi ee} &= (19.5 \pm 1.4 \pm 1.3) \text{ eV}, \\ \mathcal{B}_{\psi(2S) \rightarrow J/\psi \pi^+ \pi^-} \cdot \mathcal{B}_{J/\psi \rightarrow 2\mu} \cdot \Gamma_{\psi(2S) ee} &= \\ (45.0 \pm 1.8 \pm 2.2) \text{ eV}. \end{aligned}$$

Using the world averages value for  $\Gamma(J/\psi \rightarrow e^+e^-)$ ,  $\Gamma_{\psi(2S) \rightarrow e^+e^-}$  and  $\mathcal{B}_{J/\psi \rightarrow 2\mu}$  we derive the values  $\mathcal{B}_{J/\psi \rightarrow 4\pi} = (3.70 \pm 0.27 \pm 0.36) 10^{-3}$  and  $\mathcal{B}_{\psi(2S) \rightarrow J/\psi \pi^+ \pi^-} = 0.361 \pm 0.015 \pm 0.037$ . Figure 6 shows the  $J/\psi$  signals in the  $K^+K^-\pi^+\pi^-$  and  $K^+K^-K^+K^-$  final states, where  $233 \pm 19$  and  $38.5 \pm 6.7$  events have been observed respectively. Using the detection efficiency obtained from simulation and the effective ISR luminosity the following products have been obtained:

$$\begin{aligned} \mathcal{B}_{J/\psi \rightarrow 2K 2\pi} \cdot \Gamma_{J/\psi ee} &= (32.9 \pm 2.7 \pm 2.7) \text{ eV} \quad (12) \\ \mathcal{B}_{J/\psi \rightarrow 4K} \cdot \Gamma_{J/\psi ee} &= (3.6 \pm 0.6 \pm 0.5) \text{ eV} \quad (13) \end{aligned} \quad (14)$$

Using the world average value for  $\Gamma(J/\psi \rightarrow e^+e^-)$  we derive the relative decay rates

$$\mathcal{B}_{J/\psi \rightarrow 2K 2\pi} = (6.25 \pm 0.50 \pm 0.62) 10^{-3} \quad (15)$$

$$\mathcal{B}_{J/\psi \rightarrow 4K} = (6.9 \pm 1.2 \pm 1.1) 10^{-4} \quad (16)$$

## 5. Conclusion

A number of ISR processes have been studied with a  $90 \text{ fb}^{-1}$  data sample in the *BABAR* detector, utilizing the excellent detector efficiency and particle identification capabilities of the detector. The  $e^+e^- \rightarrow \pi^+\pi^-\pi^0$ , and preliminary  $\pi^+\pi^-\pi^+\pi^-$ ,  $K^+K^-\pi^+\pi^-$ ,  $K^+K^-K^+K^-$  cross sections cover the entire mass range from threshold to 4.5 GeV in the  $e^+e^-$  c.m. system with systematic normalization errors that are similar to those achieved by the best  $e^+e^-$  experiments over a much smaller mass region. Radiative return to the  $J/\psi$  resonance allows one to measure a number of branching fractions significantly more precisely than earlier determinations.

## REFERENCES

1. A.B. Arbuzov *et al.*, *JHEP* **9812** (1998) 9.
2. S. Binner, J.H. Kühn, K. Melnikov, *Phys. Lett. B* **459** (1999) 279.
3. M. Benayoun *et al.*, *Mod. Phys. Lett. A* **14** (1999) 2605.
4. M. Davier, S. Eidelman, A. Höcker, and

- Z. Zhang, *Eur. Phys. J. C* **27** (2003) 497;  
*Eur. Phys. J. C* **31** (2003) 503.
5. M. Davier, *The hadronic contribution to  $(g - 2)_\mu$* , these proceedings.
  6. E.P.Solodov, hep-ex/0107027.
  7. BABAR Collaboration, B. Aubert *et al.*, *Phys. Rev. D* **69** (2004) 011103.
  8. BABAR Collaboration, B. Aubert *et al.*, hep-ex/0408078, accepted by *Phys. Rev. D*.
  9. BABAR Collaboration, B. Aubert *et al.*, *Nucl. Inst. Meth. A* **479** (2002) 1.
  10. H.Cyz and J.H.Kühn, *Eur. Phys. J. C* **18** (2000) 497.
  11. A.B.Arbuzov *et al.*, *JHEP* **9710** (1997) 1.
  12. M. Caffo, H. Czyz, E. Remiddi, *Nuo. Cim.* **110A** (1997) 515; *Phys. Lett. B* **327** (1994) 369.
  13. E. Barberio, B. van Eijk and Z. Was, *Comp. Phys. Comm.* **66**(1991) 115.
  14. T. Sjostrand, *Comp. Phys. Comm.* **82** (1994) 74.
  15. S. Jadach and Z. Was, *Comp. Phys. Comm.* **85** (1995) 453.
  16. Review of Particle Physics, S. Eidelman *et al.*, *Phys. Lett. B* **592** (2004) 1.
  17. Crystal Barrel Collaboration, A.V. Anisovich *et al.*, *Phys. Lett. B* **485** (2000) 341.
  18. E852 Collaboration, P. Eugenio *et al.*, *Phys. Lett. B* **497** (2001) 190.
  19. S. Godfrey and N. Isgur, *Phys. Rev. D* **32** (1985) 189.
  20. SND Collaboration, M.N. Achasov *et al.*, *Phys. Rev. D* **66** (2002) 032001.
  21. DM2 Collaboration, A. Antonelli *et al.*, *Z. Phys. C* **56** (1992) 15.
  22. BES Collaboration, J.Z. Bai *et al.*, *Phys. Rev. D* **70** (2004) 012005.
  23. CMD-2 Collaboration, R.R. Akhmetshin *et al.*, *Phys. Lett. B* **489** (2000) 125.